

Design and Implementation of a Miniaturized Dual-wavelength UV Crosslinker

Zhiyou Wang* and Maojin Wang

School of Electronic Communication and Electrical Engineering, Changsha University,
98th Hongshan Rd, Changsha 410022, China

(Received September 6, 2021; accepted December 1, 2021; online published January 6, 2022)

Keywords: LED light source, Wi-Fi communication, uniform irradiation, palm size

To satisfy the requirement of microarray fabrication in optical sensing applications, we report a palm-sized UV LED crosslinker. By employing a microcontroller and the Wi-Fi communication technique, a sequence of different wavelengths, irradiation intensities, and crosslinking durations can be programmed by an Android app. To evaluate the irradiation uniformity of the crosslinker, we immobilized an array of fluorescent-labeled proteins on a silver substrate of high flatness by the reported crosslinker in 8 s and measured the fluorescence intensity throughout the array. For protein spots of the same concentration, the intensity difference is around 10% of the average value. The results show that the reported UV LED crosslinker can help to achieve the uniform and efficient immobilization of a protein microarray.

1. Introduction

In the past few decades, the biomolecule microarray has emerged as a high-throughput and parallel screening tool for different types of optical sensing techniques identifying biomolecular interactions, including surface plasmon resonance imaging (SPRi), fluorescence imaging, surface-enhanced Raman scattering (SERS), and chemiluminescence.^(1–4) During the identification, different reagents injected during the interactions can produce varied signal changes in spots of the microarray and their background. To maximize the contrast between the signals from the spots and their background, physical crosslinking immobilization has been widely used in microarray fabrication owing to its ability to conjugate a large amount of a reagent to a substrate in a short time.^(3–6) Currently, the most used crosslinking techniques can be categorized as chemical and physical methods. In the chemical crosslinking methods, polycondensation and polyaddition are the most common reactions for the production of polymers. The major limitation of the methods is how to optimize the reaction conditions for the highest immobilization efficiency.⁽⁵⁾ In the physical crosslinking methods, energy is transferred in the form of heat or optical radiation to the monomers, resulting in the establishment of covalent bonds among branched polymer chains.⁽⁶⁾ Owing to the advantages of a controllable duration and fewer by-products in crosslinking, the optical radiation method, i.e.,

*Corresponding author: e-mail: zywang@ccsu.edu.cn
<https://doi.org/10.18494/SAM.2022.3644>

photocrosslinking, is preferred in applications.^(7–10) Among the wavelengths of light used in the method, UV has been extensively explored in recent decades because of its low energy cost and low damage to materials.^(11,12)

Currently, most of the light sources used in the reported crosslinkers can be categorized into two types: UV lamps and UV light-emitting diodes (LEDs).^(13–19) In the UV lamp crosslinkers, although a large irradiation area can be covered by parallel distributed lamps, the low irradiation efficiency caused by heat generation and the slow response hinder their use in real-time crosslinking scenarios.⁽¹³⁾ Owing to the advantages of high luminescence efficiency, fast response, and wide wavelength range, UV LEDs have attracted much interest from academia and industry since 1998.^(14,15) Most of the commercially available UV LED crosslinkers, such as Spetroline™ Microprocessor-Controlled UV Crosslinker and LED Crosslinker 30, use a control panel to set the irradiation duration and intensity of the LEDs at a single wavelength. Compared with lamp crosslinkers, LED crosslinkers can help achieve a higher irradiation efficiency; however, their configurations limit applications requiring arbitrary irradiation sequences.^(16–18) We previously reported a Bluetooth microcontroller-based LED crosslinker in an attempt to achieve a programmable irradiation sequence. The use of the Bluetooth communication stack improved the real-time performance of the crosslinker but also brought an extra cost of the development and size of the instrument.⁽¹⁹⁾

To overcome the aforementioned shortcomings and limitations, we have developed a novel palm-sized UV LED crosslinker as reported in this paper. We discarded the Bluetooth microcontroller and instead used a regular microcontroller and Wi-Fi module to reduce the instrument size to half that in our previous work. We examined the irradiation uniformity of this crosslinker by measuring the intensity differences of a fluorophore-labeled protein array crosslinked onto a smooth silver substrate under a fluorescence scanner. For protein spots of the same concentration, the intensity difference was around 10% of the average value, which is comparable to the variation of commercially available instruments and our previous crosslinker. However, the time cost of irradiation of the palm-sized crosslinker was around 27% of that of a commercial instrument and 73% of that of our previous crosslinker. The comparison of both the irradiation uniformity and the time cost shows that the reported UV LED crosslinker can help to achieve the uniform and efficient immobilization of protein microarrays in optical sensing applications.

2. Materials and Methods

2.1 Materials

Cy3 fluorophore-labeled bovine serum albumin (Cy3-BSA) was purchased from ZSGB-bio Co. Poly(ethylene glycol) methacrylate (PEGMA) and 2-hydroxyethyl methacrylate (HEMA), monomers for the polymer layer over the silver substrate, were purchased from Sigma-Aldrich. 4-Dimethylaminopyridine (DMAP) and dimethylformamide (DMF), the acidifiers during the surface-initiated polymerization (SIP) reaction, dimethyl sulfoxide (DMSO), the solvent during the SIP reaction, 2,2'-bipyridine (Bipy), the catalyzer of the SIP reaction, and acrylic acid (AA)

were purchased from Beijing Chemical Industry Co. Ltd. Succinimidyl-ester diazine (SDA), the photocrosslinking reagent, was purchased from Qcbio Science & Technologies Co. Ltd. A BK7 substrate (Schott Glass, 75 mm × 25 mm) was purchased from Chengdu Guangming Optical Elements Co. Ltd., as used in our previous work.⁽¹⁹⁾

2.2 Methods

a) Design and implementation of crosslinker

As shown in Fig. 1, the structure of the crosslinker can be divided into two parts: an optical chamber and a control chamber. In the optical chamber, four UV LEDs at two different wavelengths (365 and 380 nm) were mounted at the top, as in our previous work, and a DHT11 temperature and humidity sensor module (product number: C117051, Aosong Co. Ltd.) was installed onto the waterproof board between the chambers.^(19,20) The control chamber is used to accommodate an LED driver adopting a 5 V–3.8 V DC step-down module and pulse width modulation (PWM) module, an STM32F103ZET6 microcontroller main control board (product number: C8287, STMicroelectronics Co. Ltd.), an ESP8266 Wi-Fi module (product number: C82891, Ai-Thinker Co. Ltd.), an MPU6050 acceleration sensor module (product number: C24112, TDK InvenSense Co. Ltd.), and a buzzer to alarm users of any abnormality of movement or temperature/humidity.

The programs running in the crosslinker include C code for the STM32F103ZET6 microcontroller and Java code for the Android app. The C code implements key tasks, such as Wi-Fi communication, LED driving, sensing data collection, and buzzer triggering. The functions of the Android app include connecting devices through the Wi-Fi function, programming the wavelength and intensity settings of the irradiation sequence, and displaying sensor data.⁽¹⁹⁾

b) Preparation of silver substrate

To evaluate the irradiation uniformity of the crosslinker, silver substrates were fabricated in accordance with our previous work.^(13,21) An atomic force microscope (AFM, Dimension icon, Veeco) was used to characterize the flatness of the silver substrate. An ESCALAB250Xi X-ray

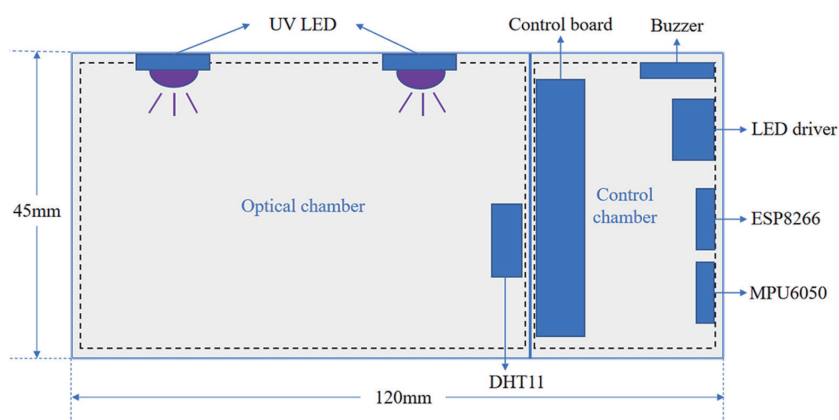


Fig. 1. (Color online) Structure of the crosslinker.

photoelectron spectroscopy (XPS) and a D/MAX-TTRIII X-ray diffractometer (XRD) were employed to analyze the elemental composition of the silver surface. After the above measurements, a polymer layer was fabricated over the silver surface by the SIP method. The carboxyl group absorbance and buffer thickness of the polymer layer were characterized as described in our previous work.⁽¹⁹⁾

c) Fabrication and test of Cy3-BSA microarray

SDA and Cy3-BSA (3, 30, 300, 3000, and 30000 ng/ml in DMSO) dissolved in DMF were printed onto the silver substrate surface to form a 5×5 microarray with one concentration for each column as in our previous work.⁽¹⁹⁾ The dried silver substrate was placed in the optical chamber of the crosslinker at room temperature. With the intensity of the LEDs set at 50%, an irradiation sequence was programmed as 2 s (365 nm)–4 s (380 nm)–2 s (365 nm).^(22–24) Lastly, the fluorescence intensity of the protein array was read under a LuxScan 10K-B fluorescence scanner.⁽²⁵⁾

3. Results and Discussion

3.1 Flatness and element analysis of silver surface

Before the SIP reaction, the flatness of an arbitrary silver substrate was examined by the AFM as shown in Fig. 2. The roughness of the sensor surface was 0.504 nm, which demonstrates that the surface of the silver substrate is smooth enough for further element analysis and polymer layer fabrication. Then, the elemental composition of the silver substrate surface was analyzed by XPS, and no metallic elements other than silver were present as shown in Fig. 3; the carbon, oxygen, and sulfur were the components in the air at the time of detection. The results of the XRD analysis in Fig. 4 confirmed that the silver surface has a clear angular composition of the

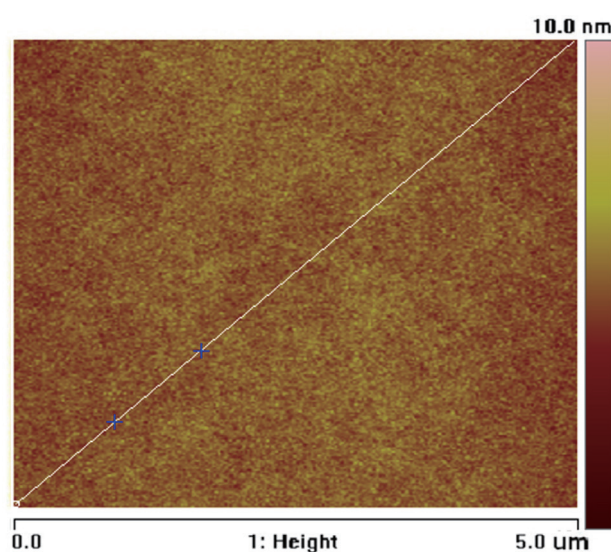


Fig. 2. (Color online) AFM result of the silver substrate surface.

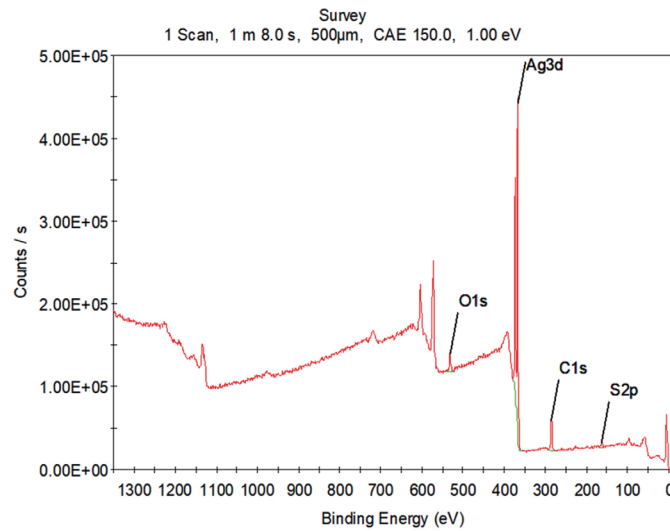


Fig. 3. (Color online) XPS result of the silver substrate surface.

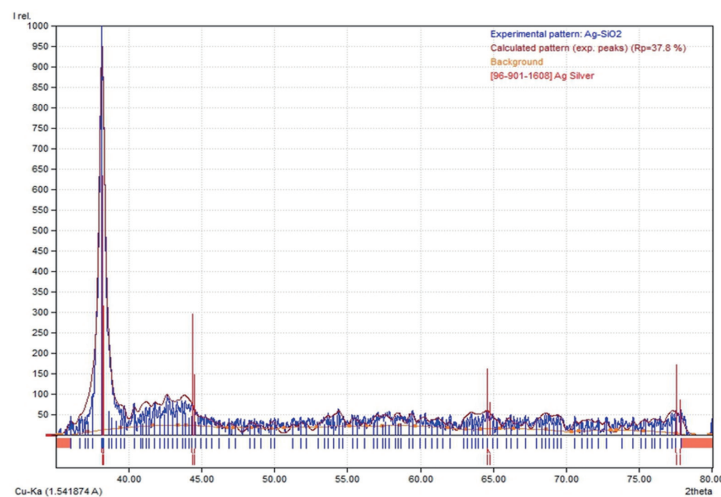


Fig. 4. (Color online) XRD result of the silver substrate surface.

diffraction from the silver element, further demonstrating that the metal surface is a pure silver structure.

3.2 Optimization of polymer layer thickness

According to Ref. 20, the largest fluorescence signal can be obtained when the thickness of the polymer layer is about 10 nm. To achieve the desired fluorescence signal, the carboxyl group absorbance and the thickness of the polymer layer were separately measured under the UV-Vis-NIR spectrophotometer and ellipsometer after different polymerization reaction durations. As shown in Table 1, when the reaction duration was 5 min, the polymer buffer layer thickness was about 10 nm. Thus, 5 min is the best choice of reaction time for the polymerization reaction.⁽²⁰⁾

Table 1

Carboxyl group density and the thickness of the polymer layer at different SIP reaction times.

	1 min	5 min	15 min	30 min	60 min
Carboxyl group absorbance (arb. units)	0.00191	0.00514	0.0159	0.0215	0.0270
Thickness (nm)	5.55	9.85	21.5	36.7	40.9

Table 2

Statistical values of Cy3-BSA fluorescence intensity at different concentrations.

	30000 ng/ml	3000 ng/ml	300 ng/ml	30 ng/ml	3 ng/ml
Average value (arb. units)	23240.16	13253.68	12160.92	9769.54	7670.62
Standard deviation (arb. units)	2290.44	1414.56	1156.36	856.48	749.74

3.3 Evaluation of irradiation uniformity

After the photocrosslinking procedure, the fluorescence signal of the Cy3-BSA array immobilized on the silver substrate was read by the fluorescence scanner. Difference and average values of the signal from the Cy3-BSA spots at the same concentration were calculated as shown in Table 2. For each concentration, the difference is around 10% of the average value, which means that the amount of protein immobilized by the crosslinker is of reasonable uniformity throughout the substrate. Branton *et al.* used Spetroline™ Microprocessor-Controlled UV Crosslinker (wavelength: 254 nm, duration: 30 s) in a double-stranded DNA immobilization on a membrane substrate for Southern Blotting.⁽¹⁶⁾ A nonuniformity of 9.63% among 24 samples was reported in their work. Moreover, similar irradiation uniformity was achieved in our previous work for an irradiation duration of 11 s.⁽¹⁹⁾ The improved crosslinking efficiency in this work can be explained as below. Owing to the use of a smaller control board, the two chambers in the palm-sized crosslinker were aligned horizontally instead of in the vertical direction in our previous work. The reduction in size increases the spatial density of the irradiation energy, which is helpful for crosslinking in a shorter duration. The above comparison shows that the irradiation of the reported crosslinker has a reasonable uniformity comparable to those of a commercially available UV LED photocrosslinker and our previous device, despite the shorter irradiation duration.

4. Conclusions

In this paper, we reported a novel palm-sized UV LED crosslinker. Different from the previously reported crosslinkers, the reported crosslinker is much smaller in size and higher in irradiation efficiency. In the evaluation of irradiation uniformity, the fluorescence signal distribution was observed throughout a fluorophore-labeled protein array immobilized on a silver substrate of high flatness and purity. Even though the crosslinking procedure was implemented in only 8 s, it achieved an irradiation uniformity comparable to reported values. This irradiation duration was at least 27% less than those of previous crosslinkers. The comparison of both the irradiation uniformity and the duration shows that the proposed palm-

sized UV LED crosslinker can be used for the immobilization of protein microarrays in optical sensing applications.

Acknowledgments

The work was supported by the National Natural Science Foundation of China (Grant No. 61905027), the Natural Science Foundation of Hunan Province (Grant No. 2019JJ50685), and the Key Research and Development Program of Hunan Province (Grant No. 2020SK2111).

References

- 1 F. S. H. Hsiao, F. R. Sutandy, G. D. Syu, Y. W. Chen, J. M. Lin, and C. S. Chen: *Sci. Rep.* **6** (2016) 28425. <https://doi.org/10.1038/srep28425>
- 2 Z. Wang, Z. Cheng, V. Singh, Z. Zheng, Y. Wang, S. Li, L. Song, and J. Zhu: *Anal. Chem.* **86** (2014) 1430. <https://doi.org/10.1021/ac402126k>
- 3 K. Yang, S. Zong, Y. Zhang, Z. Qian, Y. Liu, K. Zhu, L. Li, N. Li, Z. Wang, and Y. Cui: *ACS Appl. Mater. Interfaces* **12** (2020) 1395. <https://doi.org/10.1021/acsaami.9b19358>
- 4 J. Klupfel, R. C. Koros, K. Dehne, M. Ungerer, S. Wurstle, J. Mautner, M. Feuerherd, U. Protzer, O. Hayden, M. Elsner, and M. Seidel: *Anal. Bioanal. Chem.* **413** (2021) 5619. <https://doi.org/10.1007/s00216-021-03315-6>
- 5 I. Ahmed, H. Chen, J. Li, B. Wang, Z. Li, and G. Huang: *Compr. Rev. Food Sci. Food Saf.* **20** (2021) 5856. <https://doi.org/10.1111/1541-4337.12855>
- 6 A. Ehrmann: *Polymers* **13** (2021) 1973. <https://doi.org/10.3390/polym13121973>
- 7 P. K. Mishra, C. Yoo, E. Hong, and H. W. Rhee: *ChemBioChem* **21** (2020) 924. <https://doi.org/10.1002/cbic.201900600>
- 8 K. S. Lim, J. H. Galarraga, X. Cui, G. C. J. Linberg, J. A. Burdick, and T. B. F. Woodfield: *Chem. Rev.* **120** (2020) 10662. <https://doi.org/10.1021/acs.chemrev.9b00812>
- 9 H. Wu and J. Kohler: *Curr. Opin. Chem. Biol.* **53** (2019) 173. <https://doi.org/10.1016/j.cbpa.2019.09.002>
- 10 H. Saito, T. Goto, K. Miyajima, M. Munkjargal, T. Arakawa, and K. Mitsubayashi: *Sens. Mater.* **26** (2014) 109. <https://doi.org/10.18494/SAM.2014.948>
- 11 J. R. Hill and A. A. B. Robertson: *J. Med. Chem.* **61** (2018) 6945. <https://doi.org/10.1021/acs.jmedchem.7b01561>
- 12 P. Limpikirati, T. Liu, and R. W. Vachet: *Methods* **144** (2018) 79. <https://doi.org/10.1016/j.ymeth.2018.04.002>
- 13 S. Zhao, M. Yang, W. Zhou, B. Zhang, Z. Cheng, J. Huang, M. Zhang, Z. Wang, R. Wang, and Z. Chen: *Proc. Natl. Acad. Sci. U.S.A.* **114** (2017) E7245. <https://doi.org/10.1073/pnas.1704155114>
- 14 J. Han, H. M. Crawford, J. R. Shul, J. J. Figiel, and M. Banas: *Appl. Phys. Lett.* **73** (1998) 1688. <https://doi.org/10.1063/1.122246>
- 15 X. Deng and K. Y. Wong: *Macromol. Rapid Commun.* **30** (2009) 1570. <https://doi.org/10.1002/marc.200900183>
- 16 S. A. Branton, A. Ghorbani, B. N. Bolt, H. Fifield, L. M. Berghuis, and M. Larijani: *FASEB J.* **34** (2020) 9245. <https://doi.org/10.1096/fj.201903036RR>
- 17 C. Chen, A. Enomoto, L. Weng, T. Taki, Y. Shiraki, S. Mii, R. Ichihara, M. Kanda, M. Koike, Y. Kodera, and M. Takahashi: *Cancer Sci.* **111** (2020) 4303. <https://doi.org/10.1111/cas.14637>
- 18 W. Hu, J. Wang, I. McHardy, R. Lux, Z. Yang, Y. Li, and W. Shi: *J. Microbiol.* **50** (2012) 241. <https://doi.org/10.1007/s12275-012-1349-5>
- 19 Z. Wang and M. Wang: *Secur. Commun. Netw.* **2021** (2021) 7634982. <https://doi.org/10.1155/2021/7634982>
- 20 A. B. Kumar, J. D. Tipton, and R. Manetsch: *Chem. Comm.* **52** (2016) 2729. <https://doi.org/10.1039/c5cc09518b>
- 21 Z. Cheng, Z. Wang, D. E. Gillespie, C. Lausted, Z. Zheng, M. Yang, and J. Zhu: *Anal. Chem.* **8** (2015) 1466. <https://doi.org/10.1021/ac504110t>
- 22 J. O. Zoppe, N. C. Ataman, P. Mocny, J. Wang, J. Moraes, and H. A. Klok: *Chem. Rev.* **117** (2017) 1105. <https://doi.org/10.1021/acs.chemrev.6b00314>
- 23 S. Edmondson, V. L. Osborne, and W. T. S. Huck: *Chem. Soc. Rev.* **33** (14) 2004. <https://doi.org/10.1039/B210143M>
- 24 A. Olivier, F. Meyer, J. M. Raquez, P. Damman, and P. Dubois: *Prog. Polym. Sci.* **37** (2012) 157. <https://doi.org/10.1016/j.progpolymsci.2011.06.002>
- 25 J. E. Bradner, O. M. McPherson, and A. N. Koehler: *Nat. Protoc.* **1** (2006) 2344. <https://doi.org/10.1038/nprot.2006.282>